Evidence of Energetic Charged Particle Emission During Electrochemical Pd/D Co-deposition

M.E. Karahadian* and H.M. Doss
Department of Physics and Engineering, Point Loma Nazarene University
(Dated: April 10, 2019)

An integrative solid-state nuclear track detector (CR-39) was used to measure energetic charged particles formed during an electrochemical co-deposition of Pd/D. Tracks of alpha particles ranging in energy from 1.0 to 7.5 ± 0.5 MeV were measured. Tracks of energetic protons were observed. Evidence of triple alpha tracks appearing to originate from the same point lead to possible evidence of secondary reactions between energetic neutrons and carbon within the detector. No supporting evidence of energetic particle formations were observed for the co-deposition of Cu/D and no significant background radiation was observed on a detector in a cell filled with deionized water.

I. INTRODUCTION

It is debated whether energetic charged particles are produced during a Pd/D co-deposition process. The co-deposition process was first introduced in 1991 by Szpak et al. [1] In 2007 the first reported observations of energetic charged particle emission using this method were reported by Mosier-Boss et al. [2] who also has summarized the advantages and disadvantages of CR-39 in the context of Pd/D co-deposition [3]. Since then, this processs has been reproduced by a group at SRI International and a group at UCSD as described by Krivit & Marwin [4]. It has also been reproduced by a group at the Institute of Physics NAS of Ukraine [5]. Some have suggested that these observations are spurious results [6,7]. A question that arises in the discussion of results is the detection method. The use of Columbia Resin 39 (CR-39), a solid-state nuclear track detector (SSNTD) that is integrative over time, is commonly used to detect energetic charged particles.

In 1978, Cartwright et al. [8] were the first to demonstrate that CR-39, (composition $C_{12}H_{18}O_7$) could be used to detect particles of nuclear origin. CR-39 is formed through the polymerization of diethyleneglycol bis allycarbonate in the presence of an isopropyl peroxydicarbonate catalyst [9]. It is insensitive to electromagnetic fields and has been well characterized for protons, deuterons, tritons, alpha particles, and neutrons [10]. This detector is optically clear, amorphous, and has been manufactured in such a way that when heated, pressurized, or exposed to radiation the curing process creates a chemical bond that prevents the material from changing phase; making it a thermoset resin.

CR-39 is commonly used to detect charged particles from inertial confinement fusion (ICF) plasmas [10], as well as proton spectrometers at the National Ignition Facility [11]. Other uses include detection and characterization of cosmic particle reactions aboard the International Space Station [12] and it is commonly used for radon testing [13]. In 2014 CERN developed a passive neutron dosimeter based on CR-39 nuclear track detectors, which has been successfully tested at the CERF facility at CERN [14].

When energetic charged particles traverse through the SSNTD they leave a trail of broken bonds and free radicals. CR-39 can be used to distinguish particle energies between energies from 0.144 MeV to 19.0 MeV. [15] due to the Linear Energy Transfer (LET) function of the SSNTD. This LET function is an intrinsic property of the detector that governs the amount of energy that a charged energetic particle transfers to the material per distance. Slower particles spend more time in a given location, hence depositing more of their energy there. Faster, more energetic particles deposit less energy in a localized area they are traversing. The impacted area is more sensitive to chemical etching than the bulk substance [9]. After exposure to an etching reagent, tracks created by energetic particles in the detector can be observed with an optical microscope. The size, depth of penetration, shape, and surface luminosity provide information regarding the mass, energy and direction of motion of the incident particle just before striking the detector.

It has been suggested that the Pd/D co-deposition electrochemical cell has a highly loaded Pd lattice with deuterium, which may lead to conditions for the following fusion reactions to occur:

$$ {}^{2}_{1}\mathrm{H} + {}^{2}_{1}\mathrm{H} \longrightarrow {}^{3}_{2}\mathrm{He}\,(0.82\,\mathrm{MeV}) + {}^{1}_{0}\mathrm{n}\,(2.5\,\mathrm{MeV}) \quad (1) $$

$$ {}^{2}_{1}\mathrm{H} + {}^{2}_{1}\mathrm{H} \longrightarrow {}^{3}_{1}\mathrm{H}\,(1.01\,\mathrm{MeV}) + {}^{1}_{1}\mathrm{H}\,(3.02\,\mathrm{MeV}) \quad (2) $$

$$ {}^{2}_{1}\mathrm{H} + {}^{3}_{1}\mathrm{H} \longrightarrow {}^{4}_{2}\mathrm{He}\,(3.54\,\mathrm{MeV}) + {}^{1}_{0}\mathrm{n}\,(14.05\,\mathrm{MeV}) \quad (3) $$

$$ {}^{2}_{1}\mathrm{H} + {}^{3}_{2}\mathrm{He} \longrightarrow {}^{4}_{2}\mathrm{He}\,(3.68\,\mathrm{MeV}) + {}^{1}_{1}\mathrm{H}\,(14.62\,\mathrm{MeV}) \quad (4) $$

* mkarahadian197@pointloma.edu

Evidence of these reactions would result in tracks created within the SSNTD that display energetic alpha particles and proton tracks. Neutrons are also produced but are absent of charge, so they do not directly cause tracks as they pass through the detector. Instead, the neutrons can cause secondary reactions through interactions with detector nuclei; resulting in the production of charged particles [14]. For detection, a neutron must either scatter off of detector nuclei producing a recoil of charged particles, or undergo a neutron capture and subsequently decay into transient charged particles. These radioactive decay products can be measured.

Of the neutron interactions that may occur within the CR-39 the reaction easiest to identify is the ^{12}C(n, n')3α carbon break-up reaction.

$$^{12}_{6}\mathrm{C} + ^{1}_{0}\mathrm{n}\,(\geq 9.6\,\mathrm{MeV}) \longrightarrow 3\,^{4}_{2}\mathrm{He} + ^{1}_{0}\mathrm{n} \tag{5}$$

This reaction results in three tracks stemming from one origin. Appropriately named 'triple tracks,' these trails are a key piece of evidence that suggest DT nuclear reactions.

It is important to note that LiCl is also present in the electrochemical cell. LiCl serves as a complexing agent to form $PdCl_4$, which aids in aquation, and it serves as a background electrolyte during electrolysis. Li can also co-deposit onto the cathode with D and Pd, and if the energetic reactions listed in Eqn. 1-4 occur, then it is plausible to expect a lithium interaction. Li has the propensity to undergo the following reactions:

$$^{6}_{3}\mathrm{Li} + ^{1}_{0}\mathrm{n} \longrightarrow ^{4}_{2}\mathrm{He}\,(2.05\,\mathrm{MeV}) + ^{3}_{1}\mathrm{H}\,(2.72\,\mathrm{MeV}) \tag{6}$$

$$^{1}_{0}\mathrm{n}\,(\mathrm{fast}) + ^{7}_{3}\mathrm{Li} \longrightarrow ^{3}_{1}\mathrm{H} + ^{4}_{2}\mathrm{He} + ^{1}_{0}\mathrm{n}\,(\mathrm{slow}) \tag{7}$$

Where in the context of these nuclear reactions, fast neutrons hold energy values ranging from 1 - 20 MeV, while slow neutrons have energy of 1 - 10 eV.

II. MATERIALS AND METHODS

The butyrate electrochemical cells (1.12" × 1.125" × 2.5") were purchased from Rideout Plastics. Within the cell a polyethylene mesh (often used for cross stitch and available at craft stores) supported the cathode (99.99% Au 0.25 mm wire, Sigma-Aldrich) and anode (99.99% Pt 0.25 mm wire, Sigma Aldrich). The wires were cleaned in a 10% nitric acid solution. The upper portion of the electrodes were shrink wrapped in clear polyethylene to assure that no deposit forms on the wire above the cathode. If any deposit forms on the wire above the detector and makes contact with air-solution interface, the Pd will release the electrolytically loaded deuterium gas from the exposed deposit.

Before placing the CR-39 behind the cathode and securing it with fishing line, care was taken to remove a small corner of the polyethylene detector cover on the numbered side of the notched edge and expose it to 5 seconds of an Am-241 source [9]. This corner is used to calibrate the detector after it has been processed. On the obverse side, the lower half of the polyethylene cover was removed, and the detector was secured behind the cathode to the polyethylene mesh using fishing line. The upper half of the detector that remained in contact with the unwrapped wire still had its polyethylene cover. A bridge of the polyethylene mesh was used to secure the two mesh supports to the sides of the cell as shown in Figure 1.

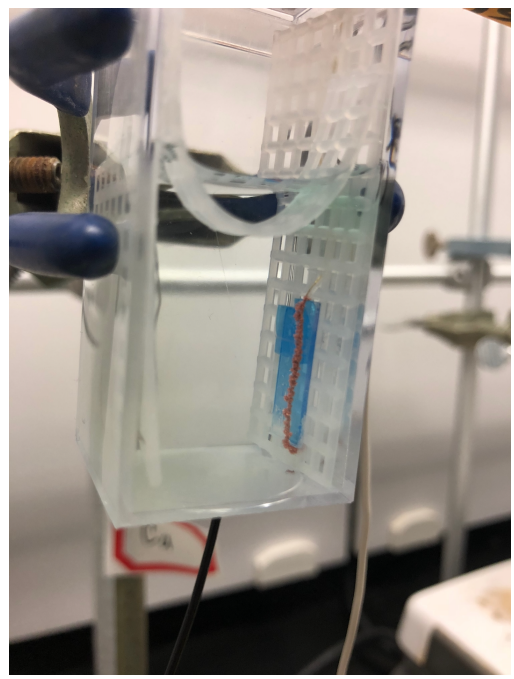

FIG. 1. Image of the copper deposit on the Au cathode during the second run in a Cu/D electrolytic cell. The cell geometry shown is similar to that which was used for all the experimental runs. The image displays the: CR-39 detector, Au cathode, Pt anode, polyethylene mesh supports and bridge.

A 0.03 M solution of $PdCl_2$ (99.9%, Pd Fisher Scientific) with 0.3M LiCl (anhydrous, free-flowing, Sigma Aldrich) in 20 mL D_2O (99.99%, Sigma Aldrich) was placed in the cell after the $PdCl_2$ dissolved. The reagents were measured using a precision weight scale (Melter, AE 240). The cells were connected in series to a constant current source (Instek, PS-6010) and a voltmeter (Keysight Technologies U3401A $4\frac{1}{2}$ Digital Dual Display Multimeter). The current was held near 0.1 mA for 24 hours, increased to roughly 0.2 mA for the next 24 hours, and then remained at approximately 0.5 mA until the solution became nearly clear (5 to 7

days). The low initial current promotes good adherence of the Pd to the Au cathode. After the solution cleared, the current is increased to 1, 5, 10, 25, 50, and 100 mA over 24 hour intervals. Figures 2-3 show the cells at the beginning and end of an experimental run. Tables S1-S3 in the supplementary section provide the date, time, current, and voltage measurements for the three Pd/D runs, as well as the control experiments.

Alongside the cell containing Pd were two control cells. One control cell followed the same set-up and procedures above but used $CuCl_2$ rather than $PdCl_2$. Palladium is sometimes referred to as a 'metal sponge' because it soaks up hydrogen similar to how a porous material would soak up water. At standard ambient temperature and pressure, palladium can absorb up to 900 times its own volume of hydrogen [16, 17]. This effect is poorly understood, yet we do know that a contributing factor is the lattice structure for Pd. Its face centered cubic parameters are: 389.07, 389.07, 389.07 pm, large enough to contain deuterium atoms (charge radius of 2.14 fm [18]).

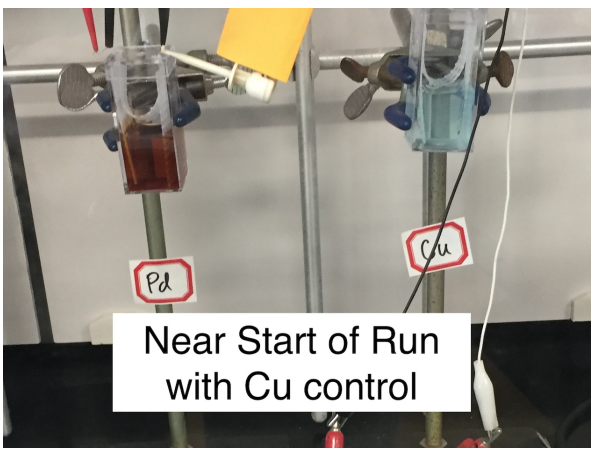

FIG. 2. Two experimental cells near the start of the second run. The darker brown color indicates aqueous Pd while the light blue is indicative of aqueous Cu. As the electrolysis is carried out palladium and copper will adhere to their respective cathodes, allowing the solutions to become more transparent as the experiment proceeds.

Copper retains similar properties, it is a face centered cubic structure with lattice parameters of 361.49, 361.49, 361.49 pm. The only significant difference between Pd/D and Cu/D is that Pd undergoes deuterium loading while Cu does not. Outside of this difference, the metal ion reduction process, electrochemical dissociation, and dendritic deposit formed are nearly congruent for both cells. The second control cell for each experimental run consisted of CR-39 with its polyethylene cover half removed (identical to the active cells), but submerged in deionized water and placed in the same hood to measure ambient radiation. The detector measuring background radiation was not vertically oriented as

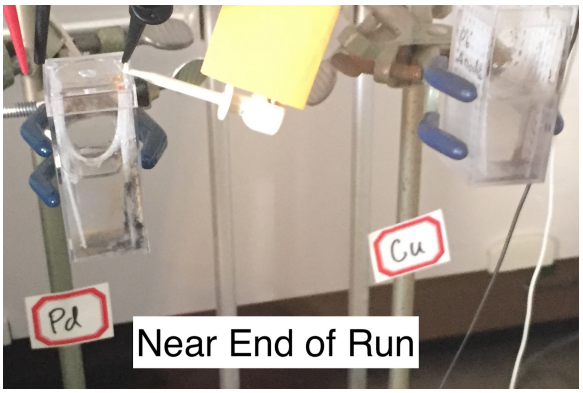

FIG. 3. Two experimental cells during the second run after the palladium and the copper have electrochemically plated out of solution.

those in the electrolytic cell, however the vertical orientation was done in previous experiments [9].

At the end of the experiment, the CR-39 was carefully removed and rinsed with deionized water. Before the CR-39 can be etched, a thermodynamically stable environment was created to control the etch rate. An Erlenmeyer flask was filled with deionized water, placed on a hotplate (Corning PC-420D), and insulated with aluminum foil as seen in Figure 4. The temperatures were recorded using a digital thermometer every half hour. Once the temperature inside the flasks reached 62-65 °C, test tubes of 6.5 M NaOH were inserted. Tables S4-S6 in the supplementary section provide the time and temperature data for each etching procedure. The detectors were etched for 7.5 hours and removed from the test tube. The detectors were then rinsed in deionized water, placed in acetic acid for 5 minutes to ensure the end of the etching process, and thoroughly rinsed again with deionized water. The detectors were then air dried and archived.

FIG. 4. To maintain a thermodynamically stable etching environment, the flasks were insulated with aluminum foil.

The CR-39 was examined using a Konus, Campus optical microscope (BM-100-FL) with 10× and 40× magnification. With IS Capture software and CCD microscope camera (Optixcam, KC110307143), dimensions of the pits were recorded. These were measured by taking the major and minor axis of elliptical tracks, or radii for normally incident particles as seen in Figure 5.

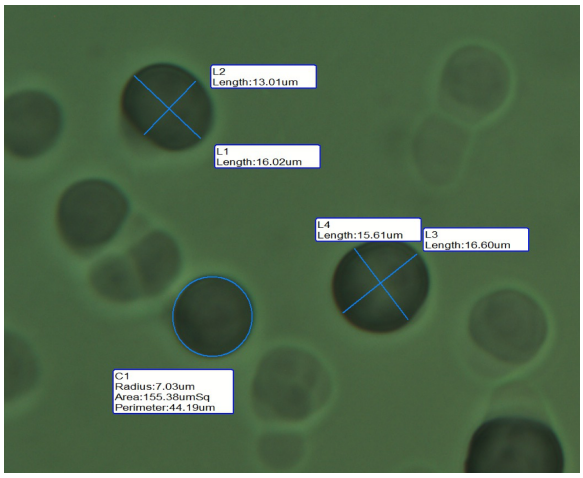

FIG. 5. Charged particles that enter the detector normal to the surface appear as circular tracks. Conversely, particles that enter the detector from angles less than 90° display an elliptical track.

Due to variations in the CR-39 manufacturing process, it is common practice to calibrate each detector by irradiating a small corner for 5 seconds with a source where the energy is known. Each run's detector was calibrated using the known energy of the alpha particles emitted by the Am-241 source (Figure 6) and *Track Test* as described below. This source could not be in direct contact with the CR-39 detector, rather there was between 1 to 3 mm of air separating it from the detector depending on the run. Energy loss estimates were taken into account when calibrating each detector. These estimates were made using *Stopping and Range of Ions in Matter* (SRIM). After the detector was etched, measurements of the pits created by the Am-241 source were used to calibrate the Pd/D alpha particle pit measurements.

In areas of high pit density, it is almost impossible to distinguish individual tracks from one another as they overlap and display an inaccurate representation of expected singular pit dimensions. Because of this, most of the data collected were in regions of less track density. It is also difficult to differentiate particle species because of the energy losses due to the distance charged particles must traverse to interact with the detector. The Pd deposit, Au wire, thin solution separation, and polyethylene layer are all regions charge particles deposit energy before finally coming to rest within the CR-39.

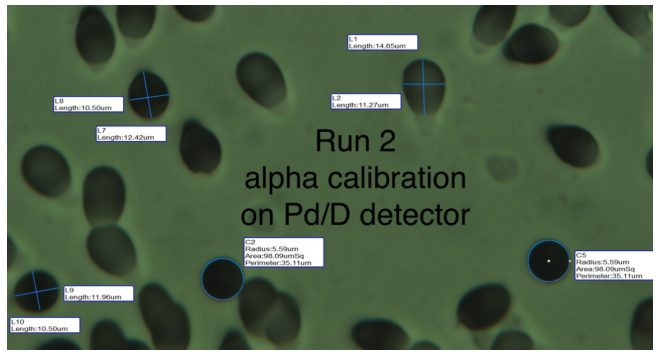

FIG. 6. 40× microscope image of Am-241 5.5 MeV alpha particle track measurements. These were used to calibrate the alpha particle energies observed within the CR-39 for each experimental run.

The pits were distinguished from superficial blemishes in a number of ways. Charged particle tracks are clean edged pits which show brighter regions deeper within the track due to internal reflection near the end of the pit. Figure 7 displays a region of the CR-39 detector where three images were taken at different focal lengths and overlaid to display optical contrast.

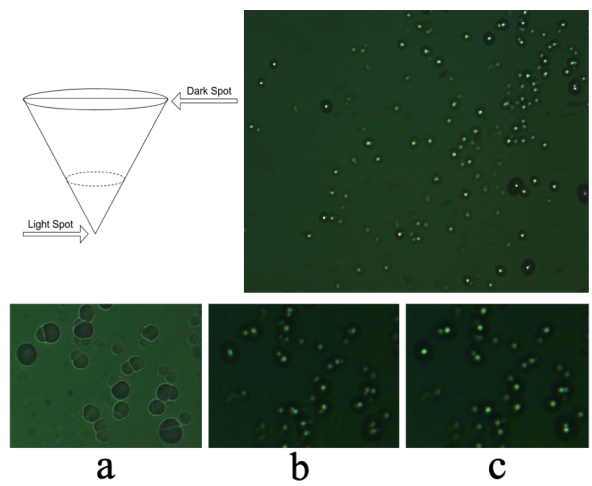

FIG. 7. 40× magnification photographs of CR-39. When the focal length is adjusted, the light from the microscope lamp reflects off the walls of the conical track resulting in a brighter region. The largest image is an overlay at three different focal lengths. Three images below show the progression of increasing focal length. **Image a** is of the shortest focal length while images **Image b** and **Image c** have longer focal lengths in increasing progression. The coalesce point becomes more refined as the focal length is increased. By doing this, maximum optical contrast may be observed.

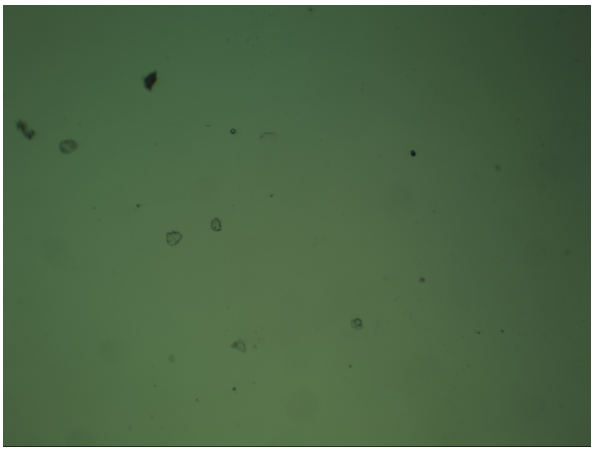

FIG. 8. Photograph of experimental Cu/D CR-39 at 10× magnification from Run 3. The image displayed shows what is typically observed following the etching procedure. The only observable markings represent superficial blemishes (e.g.scratches and dust)

III. DATA AND ANALYSIS

After each experimental run, the Pd/D CR-39 was abundant with charged particle tracks. In contrast, Figure 8 displays CR-39 used on a Cu/D experimental run where no tracks are observed. Sample measurements of approximately 45 points were taken by hand for each of the three Pd/D runs. This was done to get a relative energy approximation for the observed co-deposition generated alpha particles. Although dimensions of proton tracks were measured as seen in Figure 9, they have not yet been characterized.

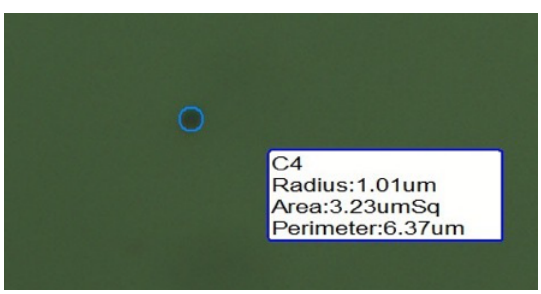

FIG. 9. Photogtraph of CR-39 at 40× magnification. A very small track oriented on the back side of the SSNTD indicates the presence of a proton. This location requires the particles detected to be considerably more energetic to traverse through the entire 200μm thick detector.

To obtain a reasonable etch rate and estimation of the charged particle energy distribution within the detector, we used *Track Test*; a program developed by Nikezic and Yu [19]. The common use of *Track Test* is to predict what charged particle dimensions (e.g. major and minor axis), appear to be within a SSNTD; provided the energy, angle of incidence, detector type, and bulk etch rate. The amount of localized damage along the track is related to the rate at which energy is lost by the particle (dE/dx where x is the distance along the track). As the etching time is increased, the diameter and depth of the track increase at the same rate. The dimensions of the pit for a given particle type are directly related to the particle's incident energy.

Track Test was first used to determine the bulk etch rate and a good fit for the pits left behind by alpha particles of a known energy (Am -241 calibration). Once a good fit was found for a CR-39 detector, tables were created of pit dimensions for various incident angles of an alpha particle with a given energy. These tables (Tables S7-S9) were constructed for each of the detectors used in the Pd runs with a 0.5 MeV step size in energy. Following the calibration tables, each of the pits measured in the Pd runs were fitted to a given energy, as shown in Table S10-S12.

Other tracks observed infer the presence of neutrons, however they are more difficult to distinguish from charged particles. Triple tracks show three separate pits stemming from one singular point. This is used to differentiate neutrons from other overlapping charged particles in CR-39. The focal length of the microscope is adjusted deeper into the track to identify if the light in each track appears to coalesce to a single point. During our experimental runs there is evidence that suggests neutron interactions as seen in Figure 10. Energetic tritons and deuterons are expected, yet are similar in size to the observed alphas and with the various interactions with materials before striking the CR-39 are not easy to distinguish.

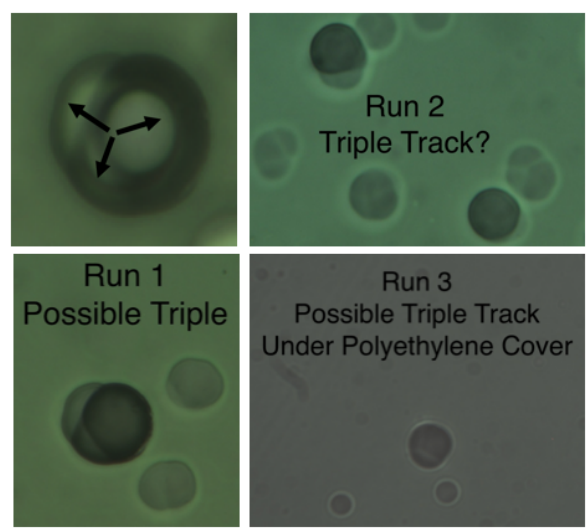

FIG. 10. From all three Pd/D experimental runs, track evidence infers the presence of neutrons. The bottom right image in the set is different from the rest in that it was photographed in a region underneath the 200μm polyethylene film. Particles found in this region are required to be considerably more energetic because of the added layer of polyethylene.

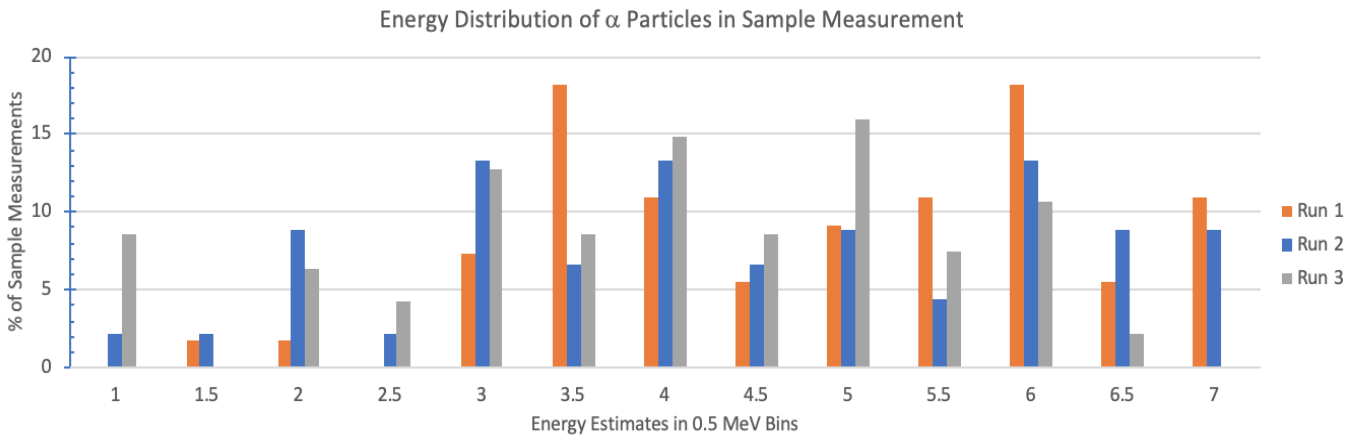

FIG. 11. Results of the qualitative analysis from the alpha particle energy distribution in CR-39.

IV. RESULTS AND DISCUSSION

The energy distribution from the small random sample of measurable tracks shows a range of incident alpha energies upon the detector from 1 to 7 MeV as seen in Figure 11. The fusion reactions (Eq. 1-4) produce alpha particles up to 3.68 MeV, provided no extra input energy. More than 50% of the measurements shown in Figure 11 for each run are greater than or equal to 4 MeV.

A side-by-side comparison of both alpha particles from the Am-241 calibration of the detector and from the Pd/D pit regions are displayed in Figure 12. The features observed by Pd/D co-deposition are consistent with those expected from authentic particle tracks [9,10]. Figure 13 from the Cu/D cell of Run 3, shows the contrast between chemical damage and a pit created from an energetic particle. The region with chemical damage shows an irregular pattern and is inconsistent with tracks produced by energetic charged particles. Finding tracks on detectors in the Cu/D cells is rare.

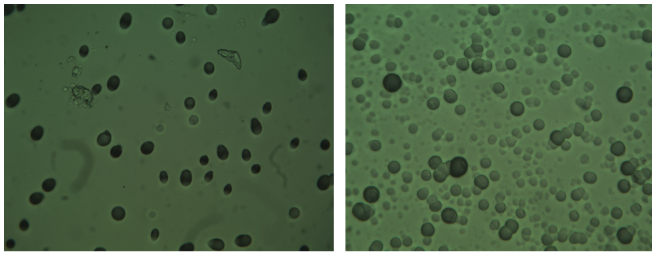

a b

FIG. 12. **Image a** is a 40× magnification snapshot from Am-241 alpha particle calibration. Most of the tracks in this image retain a similar size and optical contrast profile. **Image b** is also a 40× magnification snapshot. The tracks from this image are from the Pd/D co-deposition cell.

Shape, size and focal length differentiation are elements that we used to separate pits created by charged particle from chemical damage or superficial blemishes (e.g. scratches, dust) [4]. As a result, by varying the focal length of Figure 13 only areas of contrast are observed within the single track shown.

As discussed *vide supra*, when analyzing the tracks resultant of Pd/D co-deposition two pictures are taken. One at the surface of the pit, another by adjusting the focal length to the convergence point of the conical track.

Optical characterization of CR-39 used in Pd/D co-deposition provides evidence of energetic charged particles produced during the Pd/D electrolytic cell

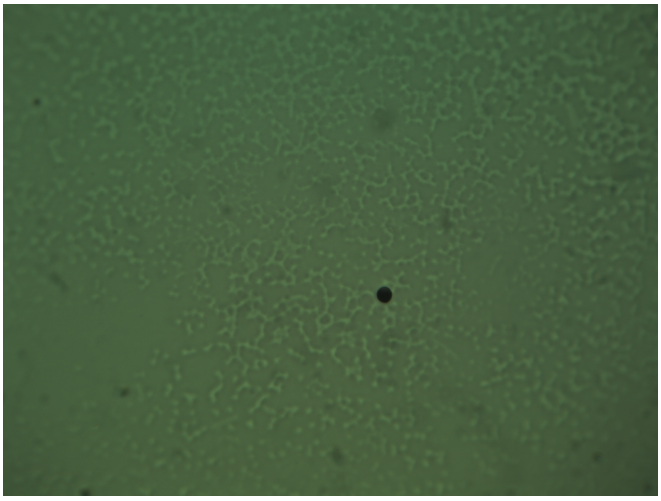

FIG. 13. Photograph taken of CR-39 at 40× magnification. Chemical damage creates this observable fractal-like pattern on the surface of the detector. This result differs significantly from tracks resultant of a charged particle.

experiments. The tracks observed are consistent with those in other experiments using CR-39 to measure nuclear byproducts [9]. The same effect was not

observed in the control experiments using both Cu/D or the detectors measuring background radiation in the laboratory area. The results in the Pd/D cell are significantly above background and show tracks made by energetic alpha particles, protons, as well as possible secondary tracks made by energetic neutron interactions.

Future works include our SSNTDs scanned by a TASL (Track Analysis Systems Ltd) scanner to gather total track counts on the detector. The TASL analysis method uses precision optics to measure the depth and axis dimensions of the tracks. As a result it ignores any overlaying tracks present, and hence ignores any possible triple tracks. The TASL imager provides energy estimates of the particles causing the tracks and an accurate identification of protons and alpha particles.

Other areas of study include analyzing the role that lithium plays within the electrolytic cells. LiCl dissociates to Li^+ similarly to how D_2O and $PdCl_2$ dissociate to D^+ and Pd^{2+} cations that adhere to the Au cathode. Due to the propensity of lithium to undergo tritium breeding, comparisons between KCl and LiCl will be analyzed.

V. ACKNOWLEDGEMENTS

We appreciate L.P. Forsley and P.A. Mosier Boss for discussions and donations of CR-39, and use of their Konus Campus optical microscope, L. Votapka for use of his lab, and the PLNU Chemistry Department for their support.

[1] Szpak, P.A. Mosier-Boss, J. J. Smith, J. Electroanal. Chem. 302 (1991)

[2] Mosier-Boss PA, Szpak S, Gordon FE, Forsley LP. Use of CR-39 in Pd/D co-deposition experiments. The European Physical Journal Applied Physics. 2007;40(3):293303.

[3] Mosier-Boss et. al. J. Condensed Matter Nucl. Sci., vol. 14, pp. 29-49 (2014)

[4] S. B. Krivet J. Marwan, J. Environ. Monit. (11) (2009)

[5] Savrasov, V. Prokopenko, E. Andreev, J. Condensed Matter Nucl. Sci. 22 (2017)

[6] L. Kowalski, Comments, Eur. Phys. J. Appl. Phys. 44, (2008)

[7] Shanahan, K.L., Comments, J. Environ. Monit. (2010)

[8] B.G. Cartwright, E.K. Shrik, P.B. Price, Nucl. Instrum. Meth 153, 457 (1978)

[9] Mosier-Boss, P. A., Szpak, S., Gordon, F. E., Forsley, L. P. Use of CR-39 in Pd/D co-deposition experiments. The European Physical Journal Applied Physics (2007)

[10] F.H. Seguin, et al. Rev. Sci. Instrum. 74, 975 (2003)

[11] H. Sio, F. H. Seguin, J. A. Frenje, M. Gatu Johnson, A. B. Zylstra, H. G. Rinderknecht, M. J. Rosenberg, C. K. Li, R. D. Petrasso, Rev. Sci. Instrum. 85 11E119 (2014)

[12] J.K. Palfalvi, Y. Akatov, L. Sajo-Bohus, J. Szabo, I. Eordogh, Cosmic Particle Induced Reaction Detection with SSNTD Stacks Exposed On-Board of the international Space Station in 10th International Conference on Nuclear Reaction Mechanisms (2003)

[13] Tata, B., Long, S. Acceptance Testing of the TASL Radon Dosimetry System. (2016)

[14] Caresana, M., Ferrarini, M., Parravicini, A., Naik, A. S. Dose measurements with CR-39 detectors at the CERF reference facility at CERN. Radiation Measurements,71 (2014).

[15] P. A. Mosier-Boss, J. Y. Dea, L. P. Forsley, M. S. Morey, J. R. Tinsley, J. P. Hurley, and F. E. Gordon, The European Physical Journal Applied Physics 51, 20901 (2010).

[16] Ralph J. Wolf, Myung W. Lee, Ricardo C. Davis, Patrick J. Fay John R. Ray, "Pressure-composition isotherms for palladium hydride," Physical Review B 48, 12415-418 (1993).

[17] Ralph J. Wolf, Khalid A. Mansour, Myung W. Lee John R. Ray, "Temperature dependence of elastic constants of embedded-atom models of palladium," Physical Review B 46, 8027-35 (1992).

[18] R. Pohl, F. Nez, T. Udem, A. Antognini, A. Beyer, H. Fleurbaey, A. Grinin, T. W. Hnsch, L. Julien, F. Kottmann, J. J. Krauth, L. Maisenbacher, A. Matveev, and F. Biraben, Metrologia 54, (2017).

[19] D. Nikezic, K.N. Yu, Mater. Sci Eng. R 46, 51 (2004)

Supplementary Materials for Evidence of Energetic Charged Particle Emission During Electrochemical Pd/D Co-deposition

Located in this section are tabulated results from the electrochemical charging procedure (S1-S3), the digital thermometer measurements from the 7.5 hour 6.5 M sodium hydroxide etching procedure (S4-S6), as well as the elliptical and circular alpha particle sample data set measurements (S7) for each of the three experimental runs. Also found in this section are the Am -241 calibration energy tables used to fit the measured Pd/D co-deposition alpha particles. The values displayed in these tables are a direct result from the output of *Track Test*.

Run 1 Electrolysis						single current loop with voltmeters in
		Across both	CR-39: Pd	CR-39: Cu	comments	paralell to cell. Current source with "Hi/Lo"
		cells	5521540	5521535		button set to Hi
Date	Time	Current (mA)	Voltage (V)	Voltage (V)		Voltmeters ingaged after current was established
9/10/18	17:27	0.103	-0.64	-0.66		
	18:05	adjusted to				
		0.15				Noticeable fluxuations between 0.130 and 0.
	18:28	0.134	-0.66	-0.62		
9/11/18	14:50	.160-190	-0.475	-0.64		upped current to 0.2mA
	22:22	.166-.186	-1.49	0.336		current droped to .166-.186
						(maybe issue with polarity?) pd plating wong side
9/12/18	9:51	0.195	0.9764	0.9888		
	20:14	0.252	0.84	0.704		reverse polarity at 15:50
9/13/18	8:42	0.151	0.567	0.959		
	12:54	0.242	0.77	0.996		
9/14/18	9:51	0.195	0.9764	0.9888		strange filb beginning to form
	15:23	0.223	0.758	0.9984		
9/15/18	9:45	0.203	0.7951	0.9999		
	10:02	0.316	0.171	0.32		
9/16/18	9:52	0.017	0.223	0.29		sudden current drop :(--> adjust to .5mA
	20:10	0.5072	0.9774	0.968		holding steady
9/17/18	10:36	0.51	1.28	1.011		
	13:46	0.5025	1.2159	1.0157		Pd solution significantly lighter today
	18:40	0.4971	1.2099	1.0225		
9/18/18	8:51	0.4825	1.2015	1.0558		no gas formation in Cu cell
9/19/18	9:50	0.477	1.2	1.1		
	15:30	0.36401	1.19	1.075		adjusted current to .5mA
	20:11	0.369	1.2069	1.0809		
9/20/18	9:10	0.47	1.28	1.145		adusted to .5mA
	14:36	0.457	1.275	1.147		
	14:40	0.5106	1.301	1.159		
9/21/18	15:40	0.469	1.35	1.32		
9/22/18	22:07	0.401	1.554	1.368		adusted to .5mA
9/23/18	12:21	0.041	0.5969	0.581		sudden current drop :(--> adjust to .5mA
	16:14	0.5468	0.8923	1.547		functionality restored?
9/24/18	13:17	0.021	0.5209	0.5485		unresponsive dials...attemping to increase to .5mA
	19:08	0.412	1.4073	1.288		increse to 0.4943mA
9/25/18	17:10	0.464	1.5484	1.0882		
	18:15	0.473	1.5531	1.0975		
	19:40	0.462	1.5522	1.0875		
9/26/18	20:09	0.452	1.9013	1.1073		adjust to 1mA
	20:32	1.0632	2.3058	1.349		
9/27/18	8:58	1.0034	2.731	1.2914		
	9:11	0.99	2.73	1.29		
	14:56	1.02	2.75	1.2		
9/28/18	14:34	1.01	2.8	1.4		the first day both cells were completely clear!
9/29/18	20:08	1.085	2.7805	1.644		increase to 5mA
	20:14	5.111	3.0676	2.304		
9/30/18	12:02	5.1026	3.1411	2.1001		signifiant gas from Au cathodes!
	15:24	5.087	3.14	2.518		
	20:00	5.05	3.137	2.5181		lincrease to 10mA
	20:11	10.081	3.3464	2.7298		
10/1/18	9:52	10	3.32	3.34		
	20:36	10.024	3.3276	3.3435		increase to 25mA
	22:54	25	3.775	3.7199		
10/2/18	9:02	25	3.77	3.68		
	15:17	24.09	3.77	3.692		
10/3/18	10:31	25	3.8	3.71		
	14:27	25.01	3.796	3.705		increase to 50mA
	15:27	50.2	4.42	4.17		
	19:43	50.21	4.414	4.1706		
10/4/18	9:12	50	4.49	4.2		
	14:30	50.06	5.4063	4.195		increase to 100mA
	14:33	100.51	5.638	5.03389		
10/3/18	10:31	25	3.8	3.71		
10/4/18	experimental run complete					turned power off

TABLE S1. Electrolysis data from the first experimental run.

RUN 2 Electrolysis	*folded obverse cover from bottom to lower notch and then cut see images	double checked Pd run that numbers are on the back side...wire on front side after the run Half covered from notch to mark on unnumbered side,* full cover on back, except top notch corner for 5 s Am	double checked after completion of Cu run that numbers are on the back side, wire on front side. Half covered from notch to mark on unnumbered side, full cover on back, except top notch corner for 5 s Am		when completed, marked edge of chip with a screw driver blade to note end of cover, cover from notch down to edge marked.	Double checked at completion of background run that numbers are on back side. Half sheet on front, marked edge with screw driver. Goes from notch down.						
		PdCl_2 0.1064g LiCl 0.2541 g		CuCl_2 0.08092 g LiCl 0.25283 g	**20 mL D2O**							
Date	Time	CR39:5521405 Current (mA) Pd	CR39:5521405 V (V) Pd	CR39:5521404 V (V) Cu		CR39: 5521397 Background in distilled water	single current loop with voltmeters in parallel to cell. Current source with "Hi/Lo" butten set to Hi					
11/18/18	14:12	.096 to .110	0.864	1.02								
	14:28	0.104										
	14:21	0.152	0.89	1.19								
	14:22	0.136	0.885	1.19								
	14:25	0.125	0.876	1.18								
	14:44	0.104	0.865	1.102								
11/19/18	8:50	0.0037	0.619	0.869								
	8:52	0.111	0.802	1.183								
	14:19	0.0614	0.7757	1.142								
	14:20	0.124	0.8065	1.255								
	14:40	0.0963	0.807	1.255								
11/20/18	10:31	0.17	0.833	1.245								
	10:33	0.187	0.839	1.25								
11/21/18	14:05	0.01643	0.819	1.238								
	14:08	0.551	1.0003	1.6317								
	14:12	0.564	1.004	1.472								
	14:14	0.568	1.0034	1.4437								
	14:22	0.561	0.9911	1.3587								
11/22/18	8:29	0.5298	0.92	1.304								
	8:30	0.5417	0.9171	1.3036								
	8:38	0.528	0.922	1.304								
	15:46	start adjusting										
	15:48	0.561	0.992	2.30								
	15:49	0.558	0.993	2.28								
	16:08	0.578	1.420	0.992								
	16:11	0.596	1.010	1.43								
	16:12	0.598	1.010	1.42								
	16:17	0.595	0.999	1.41								
10/20/18	8:51	0.612	0.920	1.35								
	14:19	0.500	0.901	1.33								
10/21/18	13:42	0.483	0.910	1.376								
10/22/18	9:51	0.586	0.961	1.49								
	14:38	0.601	0.978	1.52								
	15:22	0.600	0.986	1.51								
10/23/18	17:15	0.483	0.904	1.38								
24-Oct	15:36	0.463	1.47	2.23								
	15:40	0.483	1.47	2.28								
	16:00	0.495	1.49	2.35								
10/25/18	9:11	0.434	1.52	2.42								
	22:28	0.423	1.577	2.853								
10/26/18	12:02	0.358	1.98	2.82								
	16:06	0.362	2.05	2.86								
	16:07	0.97	2.21	2.98								
	16:11	1.01	2.25	3								
10/27/18	17:43	0.924	2.72	3.03								
	17:48	0.96	2.73	3.03								
10/28/18	10:24	0.825	2.75	2.99								
	10:26	0.809	2.75	2.99								
	10:44	0.806	2.75	3.00								
	10:45	0.813	2.75	3.00								
	12:20	0.833	2.76	3.00								
	12:21	1.005	2.78	3.03								
	15:00	0.931	2.79	3.02								
	15:02	5.176	3.0756	3.3186		oops, not clear yet						
	15:38	1.1544	2.8048	3.064		turned back down until clear						
10/29/18	9:56	1.1	2.83	3.03								
	9:57	1.097	2.83	3.03								
	15:01	1.106	2.84	3.03								
	15:02	1.107	2.84	3.03								
10/30/18	10:48	1.12	2.85	3.03								
	16:18	1.13	2.86	3.02								
	16:42	1.13	2.86	3.02								
12/3/18	14:39	50.103	4.8023	4.7975								
	14:45	100.57	6.12	6.015	turn up to 100 mA							
	15:11	100.57	6.052	5.908								
	15:11	100.58	6.098	5.928								
12/4/18	14:16	100.65	5.313	5.189								
	14:16	100.66	5.314	5.19								
	15:32	100.66	5.313	5.189	TURN OFF							

TABLE S2. Electrolysis data from the second experimental run.

Date	Time	CR39: 5521221 Current (mA) Pd	CR39: 5521221 V (V) Pd	CR39: 5521289 V (V) Cu		CR39: 5512320 Background in distilled water	single current loop with voltmeters in parallel to cell. Current source with "Hi/Lo" butten set to Hi
10/15/18	8:01	.096±10	0.876	1.23			
	8:04	0.067	0.856	1.21			
increased	? Was diminishing						
increased	20:26	0.0746	0.873	1.22			
	20:36	0.0546	0.852	1.19			
	20:41	0.0567	0.859	1.2			
	20:47	0.0536±0.01	0.853	1.196			
	20:56	0.052±0.01	0.838	1.18			
10/17/18	11:57	0.040±0.01	0.732	0.988			
	14:56	0.051±0.001	0.743	1.05			
	15:33	0.162	0.808	1.24		up current	*took some up and down adjusting over about 5 minutes
	15:37	0.156	0.805	1.25			
	15:44	0.133	0.794	1.24			
	16:05	0.115	0.788	1.23			
	16:56	0.134	0.8	1.24			
	17:00	0.13	0.796	1.24			
	17:01	0.130±0.02	0.798	1.24		fluctuation between 123 microamps and 158 microamps....most time spent around 130-135	
	17:45	0.119	0.792	1.23			
	17:46	0.122	0.803	1.24			
	17:47	0.13	0.796	1.24			
	18:26	0.122	0.790	1.24			
10/18/18	12:05	0.145	0.791	1.25			
	12:35	0.123-0.144	0.784	1.238			
	14:24	0.14	0.798	1.25			
	15:44	0.132	0.78	1.24			
	15:45	0.244	1.79	2.28		up current ugh...checked the high low button....turned to high then back to low)	
	15:48	0.262	1.41	2.21			
	15:50	0.211	1.26	1.28		adjust because cimbing to 300 microamps	
	15:51	0.195-.220	1.26	1.28			
	15:54	0.183-0.204	1.20	1.27			
	15:09	0.199	0.808	1.27		staying around 200 microamps	
10/19/18	15:12	0.209	0.825	1.286			
	15:42	0.191	0.815	1.27			
11/23/18	10:32	0.5078	0.9244	1.3134			
	10:35	0.5321	0.9408	1.3197			
	15:58	0.5307	0.9573	1.3314			
	22:12	0.5541	1.0496	1.3598			
11/24/18	9:50	0.5824	1.6761	1.3931			
	9:50	0.6055	1.6778	1.3927			
	19:28	0.5871	1.6909	1.4226			
11/25/18	23:17	0.49795	2.173	2.3532			
11/26/18	9:50	0.43689	2.1834	2.3213			
	14:38	0.45808	2.19	2.3406			
	14:53	0.474	2.196	2.346			
11/27/18	10:50	0.434	2.6042	2.8488	adjust up		
	14:47	0.4558	2.6317	2.8766			
	17:28	0.5205	2.6506	2.8946			
11/28/18	14:43	0.3912	2.6624	2.8585			
	14:43	0.3981	2.6623	2.8584			
	14:43	0.4313	2.2255	2.8277			
	14:44	0.4283	2.2266	2.8320			
	14:46	0.4626	2.5183	2.8602			
	14:47				Turn up to 1mA		
	14:49	1.0035	2.7572	2.9814			
	14:49	1.0028	2.7519	2.9820			
	14:59	0.9821	2.7723	2.9903			
	15:00	1.0066	2.7743	2.9934			
	15:00	0.9823	2.7740	2.9913			
	15:01	0.9840	2.7744	2.9919			
	15:01	0.9842	2.7747	2.9923			
	15:01	0.8879	2.7771	2.9954			
11/29/18	13:24	0.9569	2.8207	2.9997			
	14:48	0.9370	2.8200	2.9900			
	14:49	5.0168	3.1620	3.3104	turn up to 5 mA		
	14:55	5.1150	3.2094	3.3344	turn up drifting		
11/30/18	11:46	5.0950	3.1958	3.3393			
	14:46	5.075	31,950	3.3344			
	14:55	5.094	3.19	3.33			
	14:55	10.47	3.46	3.56	turn up to 10 mA		
	14:59	10.451	3.4644	3.5611			
12/1/08	14:54	10.429	3.4382	3.5473			
	15:03	25.119	3.9362	3.9973	turn up to 25mA at 3		
12/2/18	11:57	25.091	3.9517	4.03			
	15:05	25.13	3.9606	4.03			
	15:07	50.244	4.6755	4.71	turn up to 50 mA		
10/31/18	9:53	1.11	2.86	2.99			
	14:57	1.27	2.88	3.02			
	15:01	5.04	3.13	3.32			
	17:28	5.34	3.16	3.38			
	20:29	5.24	3.14	3.37			
11/1/18	9:03	5.355	3.13	3.34			
	9:03	5.353	3.13	3.34			
	11:55	5.33	3.14	3.34			
	13:24	5.222	3.13	3.32			
	14:56	5.234	3.14	3.33			
	15:00	10.18	3.34	3.54		turn up	
11/2/18	14:46	10.275	3.33	3.5			
	14:54	10.325	3.33	3.51			
	15:00	25.093	3.77	3.93		turn up	
	17:11	25.042	3.75	3.93			
11/3/18	14:55	25.063	3.76	3.95			
	15:00	50.08	4.37	4.54		turn up	
11/4/18	15:00	100.92	5.59	5.65			
	22:28	100.24	5.601	5.657			
11/5/18	10:02	100.25	5.59	5.55			
	14:45	100.24	5.68	5.62			
	15:00					off	

TABLE S3. Electrolysis data from the third experimental run.

	ETCHING RUN 1 9 October 2018		
Time	5521457 Background, Number side 5 sec Am	5521541 Americium Number side 5 sec Am	
3:51		start 64.1	
3:52	start 66.7		
4:28	67.2	67.2	
4:41	66.8	67	
4:55	66.6	66.7	
5:22	66.7	66.4	
5:57	66.4	66.4	
6:04	66.4	66.3	
6:17	66.5	66.5	
7:10	67.3	67.2	
7:29	67.7	66.7	
7:45	67.3	66.3	
8:00	67.2	65.9	
8:30	67	65.9	
8:56	67.2	66.3	
9:15	67.3	66	
9:30	67.4	65.9	
9:47	67.2	65.7	stop
	2 distill h20 rinses, 1 vinegar bath 5 min, 2 distilled H20 bath		

	ETCHING RUN 1 10 October 2018		
Time	5521535 Cu obverse side top left (not near numbers) 5 sec Am	5521540 Pd obverse side top left (not near numbers) side 5 sec Am	
11:40		start 64.5	
11:41	start 60.7		
11:50	60.7	64.9	
11:54	60.8	64.9	
11:59	60.9	65.1	
12:02	60.9	65.2	
12:04	60.9	65.2	
1:27	57.8	66.5	
1:49	61.8	66.6	
2:08	63.1	66.6	
2:40	63.2	66.2	
3:13	63.2	66.4	
3:36	63.2	66.8	
4:37	63.3	66.5	
5:14	63.3	66.5	
5:31	63.2	66.6	
5:58	63.2	66.6	
6:13	63.4	66.5	
7:11	63.4	67	end
7:13	63.1		
	2 distill h20 rinses, 1 vinegar bath 5 min, 2 distilled H20 bath		

TABLE S4. 6.5 M Sodium hydroxide etching data for the first experimental run. Included here also is the etching data for the background calibration detector done in conjunction with the first experimental run.

11/7/18	from **Cu run** rinsed with distilled on 11/5 after run. turning off analog hot plate	from **Pd run** rinsed with distilled on 11/5 after run. turning off digital hot plate		14 mL distilled water with 3.6633g of NaOH to make a 6.5 M solution	split so 7 mL solution in each		**11/8/18**	**background** run which sat in distilled water for entire time experiment. 7 mL distilled water with 1.8112 g of NaOH to make a 6.5 M solution		
	cr39 5521289	**cr39 5521221**	last time digital scale at 95.					**cr39 5521320**		
time	temp in ˚C	temp in ˚C					time	temp		
16:10	62.9	62.2	pd at 110 dig				14:55	63.2	hot plate 115	
16:12	62.5	62.5					15:00	63.8	hot plate turned to 110	
16:47	62.0	67.7	turn down to 100				15:09	63.5		
17:12	63.7	66.4					15:50	63.7		
17:54	64.9	65.5					16:53	64.1		
18:48	65.5	65.8					17:18	64.2		
19:03	65.8	65.9					21:15	64.8		
19:28	66.1	65.9					21:18	64.8		
20:14	66.1	65.8					20:07	64.9		
21:12	66.3	66.0					22:20	65.2		
22:10	66.7	66.3								
22:28	66.8	66.4								
23:06	66.9	66.4								
23:36	66.6	66.0								
23:40	66.5	65.9	end							
end 23:40										
AFTER ETCHING rinse with distilled water twice. Immerse in vinegar bath for 5 minutes, then rinse in distilled water 2 times.										

TABLE S5. 6.5 M Sodium hydroxide etching data for the second experimental run.

12/6/18	from **Cu run** rinsed with distilled water on 12/4 after run. turning off analog hot plateend of run 12/6 - rinse distilled H2O twice, soak vinegar 5 min, rinse distilled H2O tiwce.	from **Pd run** rinsed with distilled on 11/4 after run. turning off digital hot plate end of run 12/6 - rinse distilled H2O twice, soak vinegar 5 min, rinse distilled H2O tiwce.	**12/8/18**	**background** run which sat in distilled water for entire time experiment. 7 mL distilled water with 1.82709 g of NaOH to make a 6.5 M solution	
	cr39: 5521404	**cr39 5521405**		**cr39: 5521397**	
time	temp in ˚C	temp in ˚C	time	temp	
9:36	67.0	62.7	8:00	63.4	
9:47	65.0	62.4	9:00	65	
10:55	63.3	65.0	10:00	62.8	
11:38	63.9	64.5	14:06		end
13:08	64.7	64.7			
13:28	64.5	64.6			
13:47	64.3	64.6			
14:08	64.3	64.7			
15:02	65.1	65.2			
15:30	65.3	65.3			
16:59	65.2	65.1			
17:02	65.1	65.1			
17:06	65.0	65.0	done		
end			last time	done at 5:06	
AFTER ETCHING rinse with distilled water twice. Immerse in vinegar bath for 5 minutes, then rinse in distilled water 2 times.					

TABLE S6. 6.5 M Sodium hydroxide etching data for the third experimental run.

Run 1	etch rate 1.25	etch time 7.5 hours		equation 1 default	
Energy	Angle	Major	Minor	depth	radius
1	90	13.88	13.88	3.48	6.94
	85	13.86	13.86	3.47	
	80	13.8	13.79	3.42	
	75	13.69	13.67	3.34	
	70	13.53	13.49	3.23	
	65	13.32	13.26	3.09	
	60	13.06	12.97	2.92	
	55	12.74	12.62	2.72	
	50	12.37	12.18	2.5	
	45	11.93	11.67	2.25	
	40	11.42	11.05	1.98	
	35	10.83	10.32	1.69	
	30	10.14	9.45	1.39	
	average	12.65923077	12.47769231	2.729230769	

Run 1	etch rate 1.25	etch time 7.5 hours		equation 1 default	
Energy	Angle	Major	Minor	depth	radius
2	90	15.8	15.79	6.9	7.8975
	85	15.81	15.78	6.87	
	80	15.85	15.73	6.77	
	75	15.91	15.68	6.61	
	70	15.98	15.59	6.39	
	65	16.04	15.45	6.11	
	60	16.07	15.26	5.77	
	55	16.06	15	5.37	
	50	15.99	14.66	4.93	
	45	15.83	14.22	4.43	
	40	15.58	13.63	3.89	
	35	15.2	12.88	3.31	
	30	14.66	11.92	2.69	
	average	15.75230769	14.7376923	5.387692308	

Run 1	h rate 1	etch time 7.5 hours		equation 1 default	
Energy	Angle	Major	Minor	depth	radius
3	90	14.49	14.48	10.92	7.2425
	85	14.54	14.47	10.87	
	80	14.71	14.44	10.71	
	75	14.99	14.38	10.45	
	70	15.4	14.3	10.08	
	65	15.95	14.19	9.62	
	60	16.62	14.05	9.06	
	55	17.33	13.88	8.4	
	50	18	13.67	7.66	
	45	18.55	13.43	6.84	
	40	18.92	13.12	5.95	
	35	19.09	12.67	4.98	
	30	19	11.96	3.96	
	average	16.73769231	13.7723077	8.423076923	

Run 1	etch rate 1.25	etch time 7.5 hours		equation 1 default	
Energy	Angle	Major	Minor	depth	radius
4	90	13.12	13.11	15.33	6.5575
	85	13.15	13.09	15.26	
	80	13.28	13.04	15.02	
	75	13.51	12.95	14.63	
	70	13.83	12.82	14.09	
	65	14.27	12.64	13.4	
	60	14.85	12.42	12.57	
	55	15.6	12.13	11.6	
	50	16.5	11.77	10.5	
	45	17.8	11.32	9.28	
	40	19.41	10.77	7.95	
	35	21.22	10.08	6.52	
	30	22.46	9.26	5.01	
	average	16.07692308	11.9538462	11.62769231	

Run 1	etch rate 1.25	etch time 7.5 hours		equation 1 default	
Energy	Angle	Major	Minor	depth	radius
1.5	90	15.39	15.39	5.1	7.695
	85	15.38	15.38	5.09	
	80	15.34	15.32	5.1	
	75	15.26	15.21	4.9	
	70	15.16	15.6	4.73	
	65	15.02	14.85	4.53	
	60	14.85	14.59	4.28	
	55	14.63	14.25	4	
	50	14.36	13.83	3.66	
	45	14.02	13.32	3.3	
	40	13.6	12.68	3	
	35	13.08	11.91	2.4	
	30	12.44	10.96	2.03	
	average	14.50230769	14.09923077	4.009230769	

Run 1	etch rate 1.25	etch time 7.5 hours		equation 1 default	
Energy	Angle	Major	Minor	depth	radius
2.5	90	15.27	15.26	8.84	7.6325
	85	15.32	15.26	8.81	
	80	15.48	15.23	8.68	
	75	15.73	15.19	8.47	
	70	16.05	15.12	8.19	
	65	16.4	15.03	7.82	
	60	16.74	14.92	7.37	
	55	17.03	14.77	6.85	
	50	17.26	14.55	6.27	
	45	17.39	14.25	5.62	
	40	17.39	13.81	4.91	
	35	17.22	13.17	4.15	
	30	16.86	12.27	3.35	
	average	16.47230769	14.5253846	6.871538462	

Run 1	h rate 1	etch time 7.5 hours		equation 1 default	
Energy	Angle	Major	Minor	depth	radius
3.5	90	13.77	13.76	13.09	6.8825
	85	13.81	13.75	13.03	
	80	13.96	13.7	12.84	
	75	14.21	13.62	12.51	
	70	14.58	13.51	12.06	
	65	15.09	13.37	11.49	
	60	15.75	13.18	10.8	
	55	16.61	12.95	10	
	50	17.68	12.66	9.08	
	45	18.87	12.32	8.07	
	40	19.9	11.91	6.97	
	35	20.61	11.44	5.78	
	30	20.95	10.87	4.53	
	average	16.59923077	12.8492308	10.01923077	

Run 1	etch rate 1.25	etch time 7.5 hours		equation 1 default	
Energy	Angle	Major	Minor	depth	radius
4.5	90	12.49	12.48	17.57	6.2425
	85	12.52	12.46	17.49	
	80	12.64	12.4	17.21	
	75	12.84	12.3	16.75	
	70	13.13	12.15	16.11	
	65	13.53	11.95	15.29	
	60	14.04	11.69	14.31	
	55	14.69	11.35	13.16	
	50	15.52	10.94	11.86	
	45	16.57	10.41	10.42	
	40	17.94	9.73	8.85	
	35	19.76	8.86	7.16	
	30	22.24	7.72	5.37	
	average	15.22384615	11.1107692	13.19615385	

Run 1	etch rate 1.25	etch time 7.5 hours		equation 1 default	
Energy	Angle	Major	Minor	depth	radius
5	90	11.83	11.83	19.78	5.915
	85	11.87	11.8	19.69	
	80	11.98	11.74	19.36	
	75	12.16	11.63	18.83	
	70	12.43	11.46	18.08	
	65	12.78	11.23	17.13	
	60	13.25	10.94	15.99	
	55	13.84	10.56	14.66	
	50	14.57	10.09	13.15	
	45	15.49	9.48	11.47	
	40	16.66	8.69	9.64	
	35	18.16	7.64	7.68	
	30	20.18	6.21	5.59	
	avg	14.24615385	10.2538462	14.69615385	

Run 1	etch rate 1.25	etch time 7.5 hours		equation 1 default	
Energy	Angle	Major	Minor	depth	radius
6	90	10.38	10.37	11.36	5.1875
	85	10.4	10.34	11.29	
	80	10.49	10.26	11.06	
	75	10.64	10.11	10.66	
	70	10.86	9.9	10.12	
	65	11.15	9.62	9.43	
	60	11.53	9.24	8.59	
	55	12	8.75	7.62	
	50	12.58	8.12	6.52	
	45	13.31	7.3	5.29	
	40	14.21	6.18	3.96	
	35	15.33	4.57	2.52	
	30	12.22	2.74	1.29	
	average	11.93076923	8.26923077	7.67	

Run 1	etch rate 1.25	etch time 7.5 hours		equation 1 default	
Energy	Angle	Major	Minor	depth	radius
7	90	8.76	8.75	6.55	4.3775
	85	8.78	8.72	6.49	
	80	8.85	8.62	6.31	
	75	8.97	8.43	6.01	
	70	9.15	8.16	5.59	
	65	9.37	7.79	5.06	
	60	9.67	7.29	4.42	
	55	10.03	6.63	3.67	
	50	10.49	5.74	2.83	
	45	11.04	4.47	1.89	
	40	9.78	2.63	9.18	
	35	5.95	1.13	3.02	
	30	2.28	2.4	3.92	
	average	8.701538462	6.21230769	4.995384615	

Run 1	etch rate 1.25	etch time 7.5 hours		equation 1 default	
Energy	Angle	Major	Minor	depth	radius
5.5	90	11.13	11.12	15.56	5.5625
	85	11.16	11.1	15.48	
	80	11.25	11.02	15.19	
	75	11.42	10.89	14.72	
	70	11.67	10.71	14.07	
	65	11.99	10.45	13.23	
	60	12.41	10.12	12.23	
	55	12.94	9.69	11.06	
	50	13.59	9.15	9.73	
	45	14.41	8.45	8.26	
	40	15.43	7.52	6.66	
	35	16.72	6.25	4.93	
	30	17.33	4.44	3.12	
	average	13.18846154	9.30076923	11.09538462	

Run 1	etch rate 1.25	etch time 7.5 hours		equation 1 default	
Energy	Angle	Major	Minor	depth	radius
6.5	90	9.58	9.57	8.6	4.7875
	85	9.6	9.55	8.56	
	80	9.68	9.45	8.35	
	75	9.82	9.29	8.01	
	70	10.02	9.05	7.54	
	65	10.28	8.73	6.94	
	60	10.61	8.3	6.21	
	55	11.03	7.73	5.37	
	50	11.54	7	4.41	
	45	12.18	6	3.35	
	40	12.96	4.57	2.19	
	35	10.89	2.69	1.07	
	30	7.2	1.29	4.12	
	average	10.41461538	7.17076923	5.747692308	

TABLE S7. Energy tables created for the first experimental run.

Run 2	etch rate 1.2	etch time 7.5 hours		equation 1 default	
Energy	Angle	Major	Minor	depth	radius
1	90	13.51	13.51	3.49	6.755
	85	13.49	13.49	3.47	
	80	13.43	13.42	4.42	
	75	13.32	13.3	3.34	
	70	13.17	13.14	3.23	
	65	13.32	13.26	3.09	
	60	12.73	12.64	2.92	
	55	12.43	12.29	2.72	
	50	12.08	11.88	2.50	
	45	11.66	11.37	2.25	
	40	11.18	10.78	1.98	
	35	10.62	10.07	1.69	
	30	9.96	9.23	1.39	

Run 2	etch rate 1.2	etch time 7.5 hours		equation 1 default	
Energy	Angle	Major	Minor	depth	radius
2	90	15.18	15.18	6.90	7.59
	85	15.20	15.16	6.87	
	80	15.26	15.14	6.78	
	75	15.34	15.08	6.61	
	70	15.44	15.00	6.40	
	65	15.53	14.87	6.11	
	60	15.60	14.71	5.78	
	55	15.63	14.47	5.38	
	50	15.59	14.16	4.93	
	45	15.48	13.75	4.44	
	40	15.27	13.21	3.89	
	35	14.93	12.50	3.31	
	30	14.44	11.58	2.70	

Run 2	etch rate 1.2	etch time 7.5 hours		equation 1 default	
Energy	Angle	Major	Minor	depth	radius
3	90	13.88	13.87	10.92	6.9375
	85	13.91	13.85	10.87	
	80	14.08	13.82	10.72	
	75	14.34	13.76	10.45	
	70	14.74	13.68	10.09	
	65	15.23	13.57	9.62	
	60	15.93	13.43	9.06	
	55	16.68	13.26	8.41	
	50	17.41	13.06	7.67	
	45	18.04	12.82	6.85	
	40	18.45	12.52	5.95	
	35	18.72	12.11	4.99	
	30	18.70	11.47	3.97	

Run 2	etch rate 1.2	etch time 7.5 hours		equation 1 default	
Energy	Angle	Major	Minor	depth	radius
4	90	12.57	12.56	15.33	6.2825
	85	12.6	12.54	15.26	
	80	12.73	12.49	15.03	
	75	12.94	12.41	14.64	
	70	13.25	12.28	14.10	
	65	13.67	12.11	13.40	
	60	14.21	11.89	12.57	
	55	14.92	11.61	11.60	
	50	15.82	11.26	10.50	
	45	16.98	10.82	9.29	
	40	18.5	10.28	7.96	
	35	20.39	9.59	6.53	
	30	21.92	8.75	5.01	

Run 2	etch rate 1.2	etch time 7.5 hours		equation 1 default	
Energy	Angle	Major	Minor	depth	radius
1.5	90	14.90	14.90	5.11	7.45
	85	14.89	14.88	5.08	
	80	14.85	14.83	5.02	
	75	14.79	14.73	4.90	
	70	14.71	14.59	4.74	
	65	14.59	14.40	4.53	
	60	14.45	14.15	4.28	
	55	14.25	13.83	4.00	
	50	14.02	13.44	3.67	
	45	13.71	12.95	3.30	
	40	13.32	12.34	2.91	
	35	12.84	11.60	2.49	
	30	12.23	10.68	2.04	

Run 2	etch rate 1.2	etch time 7.5 hours		equation 1 default	
Energy	Angle	Major	Minor	depth	radius
2.5	90	14.62	14.61	8.84	7.3075
	85	14.66	14.6	8.81	
	80	14.82	14.58	8.68	
	75	15.08	14.53	8.47	
	70	15.42	14.47	8.19	
	65	15.64	14.42	7.97	
	60	16.18	14.28	7.37	
	55	16.52	14.14	6.85	
	50	16.8	13.94	6.27	
	45	16.97	13.68	5.62	
	40	17.02	13.28	4.91	
	35	16.91	12.7	4.15	
	30	16.6	11.86	3.35	

Run 2	etch rate 1.2	etch time 7.5 hours		equation 1 default	
Energy	Angle	Major	Minor	depth	radius
3.5	90	13.19	13.18	13.09	6.5925
	85	13.22	13.16	13.03	
	80	13.37	13.12	12.84	
	75	13.61	13.05	12.52	
	70	13.96	12.94	12.07	
	65	14.44	12.80	11.49	
	60	15.06	12.62	10.80	
	55	15.87	12.39	10.00	
	50	16.90	12.11	9.09	
	45	18.13	11.76	8.07	
	40	19.29	11.35	6.97	
	35	20.13	10.86	5.78	
	30	20.58	10.31	4.52	

Run 2	etch rate 1.2	etch time 7.5 hours		equation 1 default	
Energy	Angle	Major	Minor	depth	radius
4.5	90	11.97	11.96	17.57	5.9825
	85	12	11.94	17.49	
	80	12.11	11.88	17.21	
	75	12.31	11.78	16.75	
	70	12.58	11.64	16.11	
	65	12.96	11.45	15.30	
	60	13.44	11.19	14.31	
	55	14.06	10.87	13.17	
	50	14.84	10.47	11.87	
	45	15.84	9.95	10.43	
	40	17.11	9.30	8.86	
	35	18.81	8.44	7.17	
	30	21.13	7.31	5.38	

Run 2	etch rate 1.2	etch time 7.5 hours		equation 1 default	
Energy	Angle	Major	Minor	depth	radius
5	90	11.34	11.34	19.77	5.67
	85	11.37	11.31	19.68	
	80	11.47	11.25	19.36	
	75	11.65	11.13	18.82	
	70	11.9	10.97	18.08	
	65	12.24	10.75	17.13	
	60	12.68	10.47	15.98	
	55	13.24	10.11	14.65	
	50	13.93	9.64	13.14	
	45	14.81	9.05	11.47	
	40	15.91	8.29	9.64	
	35	17.32	7.27	7.68	
	30	19.19	5.85	5.59	

Run 2	etch rate 1.2	etch time 7.5 hours		equation 1 default	
Energy	Angle	Major	Minor	depth	radius
6	90	9.95	9.94	10.65	4.9725
	85	9.96	9.91	10.58	
	80	10.05	9.83	10.36	
	75	10.20	9.69	9.99	
	70	10.41	9.49	9.48	
	65	10.69	9.21	8.82	
	60	11.04	8.85	8.03	
	55	11.49	8.38	7.11	
	50	12.05	7.77	6.06	
	45	12.73	6.97	4.90	
	40	13.58	5.87	3.63	
	35	14.64	4.3	2.27	
	30	11.43	2.49	1.11	

Run 2	etch rate 1.2	etch time 7.5 hours		equation 1 default	
Energy	Angle	Major	Minor	depth	radius
7	90	8.4	8.4	6.19	4.2
	85	8.41	8.36	6.13	
	80	8.48	8.26	5.96	
	75	8.6	8.08	5.68	
	70	8.76	7.82	5.28	
	65	8.98	7.47	4.77	
	60	9.26	6.98	4.16	
	55	9.61	6.34	3.45	
	50	10.04	5.48	2.64	
	45	10.56	4.23	1.74	
	40	9.25	2.43	0.81	
	35	5.36	0.97	0.24	
	30	1.61	0.14	0.19	

Run 2	etch rate 1.2	etch time 7.5 hours		equation 1 default	
Energy	Angle	Major	Minor	depth	radius
5.5	90	10.67	10.66	14.32	5.3325
	85	10.69	10.63	14.24	
	80	10.79	10.56	13.98	
	75	10.94	10.44	13.54	
	70	11.18	10.26	12.93	
	65	11.49	10.01	12.15	
	60	11.89	9.69	11.21	
	55	12.39	9.28	10.12	
	50	13.01	8.75	8.88	
	45	13.79	8.07	7.50	
	40	14.75	7.17	6.00	
	35	15.97	5.93	4.39	
	30	16.47	4.15	2.68	

Run 2	etch rate 1.2	etch time 7.5 hours		equation 1 default	
Energy	Angle	Major	Minor	depth	radius
6.5	90	9.19	9.18	8.12	4.5925
	85	9.2	9.15	8.06	
	80	9.28	9.06	7.87	
	75	9.41	8.9	7.54	
	70	9.60	8.67	7.10	
	65	9.85	8.36	6.52	
	60	10.16	7.94	5.83	
	55	10.56	7.4	5.03	
	50	11.05	6.68	4.12	
	45	11.65	5.72	3.11	
	40	12.39	4.32	2.01	
	35	10.25	2.47	9.48	
	30	6.47	1.1	0.33	

TABLE S8. Energy tables created for the second experimental run.

run 3	etch rate 1.1				
equ 3	data rad 3.8 maj avg 7.65 run 3				
Energy	Angle	Major	Minor	depth	radius
1	90	10.70	10.70	2.63	5.35
	85	10.69	10.68	2.61	
	80	10.64	10.61	2.56	
	75	10.55	10.48	2.48	
	70	10.43	10.30	2.37	
	65	10.26	10.06	2.23	
	60	10.05	9.76	2.07	
	55	9.79	9.38	1.87	
	50	9.46	8.91	1.65	
	45	9.05	8.34	1.41	
	40	8.55	7.65	1.15	
	35	7.93	6.79	0.88	
	30				
	25				
	20				

run 3	etch rate 1.1				
equ 3	data rad 3.8 maj avg 7.65 run 3				
Energy	Angle	Major	Minor	depth	radius
2	90	11.84	11.83	5.47	5.92
	85	11.86	11.82	5.44	
	80	11.94	11.77	5.34	
	75	12.05	11.68	5.18	
	70	12.20	11.56	4.96	
	65	12.35	11.40	4.68	
	60	12.49	11.18	4.34	
	55	12.59	10.89	3.95	
	50	12.63	10.52	3.51	
	45	12.57	10.03	3.02	
	40	12.38	9.39	2.49	
	35	12.02	8.53	1.92	
	30	11.41	7.36	1.33	
	25	10.42	5.66	0.73	
	20				

run 3	etch rate 1.1				
equ 3	data rad 3.8 maj avg 7.65 run 3				
Energy	Angle	Major	Minor	depth	radius
3	90	10.95	10.94	8.81	5.47
	85	10.98	10.92	8.77	
	80	11.08	10.87	8.61	
	75	11.26	10.78	8.34	
	70	11.52	10.65	7.98	
	65	11.86	10.48	7.51	
	60	12.30	10.25	6.95	
	55	12.84	9.96	6.30	
	50	13.49	9.59	5.56	
	45	14.19	9.13	4.75	
	40	14.84	8.53	3.86	
	35	15.24	7.75	2.92	
	30	15.25	6.65	1.92	
	25	14.03	4.88	0.90	
	20				

run 3	etch rate 1.1				
equ 3	data rad 3.8 maj avg 7.65 run 3				
Energy	Angle	Major	Minor	depth	radius
4	90	9.63	9.62	12.25	4.81
	85	9.65	9.60	12.18	
	80	9.74	9.53	11.95	
	75	9.88	9.42	11.56	
	70	10.10	9.25	11.02	
	65	10.38	9.02	10.34	
	60	10.75	8.72	9.51	
	55	11.22	8.34	8.55	
	50	11.80	7.86	7.46	
	45	12.53	7.23	6.25	
	40	13.43	6.41	4.93	
	35	14.58	5.29	3.52	
	30	14.23	3.84	2.07	
	25	12.05	2.67	0.90	
	20				

run 3	etch rate 1.1				
equ 3	data rad 3.8 maj avg 7.65 run 3				
Energy	Angle	Major	Minor	depth	radius
1.5	90	11.71	11.7	3.97	5.85
	85	11.71	11.69	3.95	
	80	11.70	11.62	3.88	
	75	11.70	11.52	3.76	
	70	11.68	11.37	3.60	
	65	11.63	11.16	3.39	
	60	11.55	10.89	3.15	
	55	11.43	10.54	2.86	
	50	11.23	10.10	2.54	
	45	10.96	9.55	2.18	
	40	10.57	8.85	1.80	
	35	10.05	7.96	1.39	
	30	9.32	6.81	0.97	
	25				
	20				

run 3	etch rate 1.1				
equ 3	data rad 3.8 maj avg 7.65 run 3				
Energy	Angle	Major	Minor	depth	radius
2.5	90	11.48	11.47	7.10	5.74
	85	11.51	11.45	7.06	
	80	11.62	11.41	6.94	
	75	11.80	11.33	6.73	
	70	12.05	11.21	6.44	
	65	12.37	11.05	6.07	
	60	12.74	10.84	5.63	
	55	13.14	10.58	5.11	
	50	13.50	10.24	4.53	
	45	13.77	9.80	3.89	
	40	13.89	9.23	3.19	
	35	13.81	8.45	2.45	
	30	13.43	7.32	1.67	
	25	12.56	5.56	0.86	
	20				

run 3	etch rate 1.1				
equ 3	data rad 3.8 maj avg 7.65 run 3				
Energy	Angle	Major	Minor	depth	radius
3.5	90	10.32	10.31	10.56	5.16
	85	10.35	10.30	10.50	
	80	10.45	10.24	10.31	
	75	10.61	10.14	9.99	
	70	10.85	9.99	9.53	
	65	11.16	9.79	8.96	
	60	11.57	9.53	8.27	
	55	12.09	9.20	7.47	
	50	12.74	8.78	6.56	
	45	13.52	8.25	5.55	
	40	14.53	7.56	4.46	
	35	15.66	6.66	3.29	
	30	16.58	5.42	2.06	
	25	13.44	3.87	0.90	
	20				

run 3	etch rate 1.1				
equ 3	data rad 3.8 maj avg 7.65 run 3				
Energy	Angle	Major	Minor	depth	radius
4.5	90	8.88	8.87	9.78	4.44
	85	8.90	8.85	9.73	
	80	8.98	8.77	9.52	
	75	9.11	8.64	9.18	
	70	9.30	8.45	8.71	
	65	9.56	8.19	8.10	
	60	9.88	7.85	7.38	
	55	10.29	7.41	6.53	
	50	10.81	6.83	5.57	
	45	11.44	6.08	4.51	
	40	12.23	5.05	3.35	
	35	12.31	3.64	2.12	
	30				
	25				
	20				

run 3	etch rate 1.1				
equ 3	data rad 3.8 maj avg 7.65 run 3				
Energy	Angle	Major	Minor	depth	radius
5	90	8.10	8.09	7.13	4.05
	85	8.12	8.07	7.08	
	80	8.19	7.98	6.90	
	75	8.31	7.83	6.61	
	70	8.47	7.61	6.21	
	65	8.70	7.31	5.69	
	60	8.98	6.91	5.07	
	55	9.34	6.39	4.35	
	50	9.79	5.70	3.54	
	45	10.34	4.76	2.63	
	40	10.69	3.41	1.64	
	35				
	30				
	25				
	20				

run 3	etch rate 1.1				
equ 3	data rad 3.8 maj avg 7.65 run 3				
Energy	Angle	Major	Minor	depth	radius
5.5	90	7.29	7.29	5.18	3.65
	85	7.31	7.26	5.14	
	80	7.37	7.16	4.98	
	75	7.47	6.98	4.73	
	70	7.62	6.73	4.38	
	65	7.81	6.38	3.93	
	60	8.06	5.91	3.39	
	55	8.36	5.27	2.76	
	50	8.74	4.40	2.04	
	45	9.21	3.12	1.25	
	40	6.65	1.74	0.58	
	35				
	30				
	25				
	20				

run 3	etch rate 1.1				
equ 3	data rad 3.8 maj avg 7.65 run 3				
Energy	Angle	Major	Minor	depth	radius
7.5	90	4.18	4.17	1.33	2.09
	85	4.19	4.12	1.29	
	80	4.22	3.93	1.18	
	75	4.27	3.59	1.00	
	70	4.34	3.03	0.75	
	65				
	60				
	55				
	50				
	45				
	40				
	35				
	30				
	25				
	20				

run 3	etch rate 1.1				
equ 3	data rad 3.8 maj avg 7.65 run 3				
Energy	Angle	Major	Minor	depth	radius
5.25	90	7.69	7.68	6.06	3.8425
	85	7.71	7.66	6.01	
	80	7.78	7.57	5.85	
	75	7.89	7.40	5.58	
	70	8.15	7.17	5.20	
	65	8.25	6.84	4.73	
	60	8.51	6.41	4.14	
	55	8.85	5.84	3.48	
	50	9.25	5.06	2.72	
	45	9.76	3.98	1.87	
	40	8.63	2.52	1.02	
	35				
	30				
	25				

run 3	etch rate 1.1				
equ 3	data rad 3.8 maj avg 7.65 run 3				
Energy	Angle	Major	Minor	depth	radius
6	90	6.48	6.47	3.75	3.24
	85	6.49	6.44	3.71	
	80	6.55	6.32	3.57	
	75	6.63	6.12	3.35	
	70	6.76	5.83	3.03	
	65	6.92	5.41	2.63	
	60	7.13	4.83	2.15	
	55	7.39	4.02	1.58	
	50	7.71	2.82	0.95	
	45				
	40				
	35				
	30				
	25				
	20				

TABLE S9. Energy tables created for the third experimental run.

Run 1 Etch 9 Oct 2019. etch time =7.5h					
Pd:5512540					
		R1 TRACKS			
	radius	Energy	major axis	minor axis	Energy
1	7.13	3	20.99	19.83	
2	3.28	N/A	14.38	13.57	3.5
3	3.18	N/A	18.79	16.13	N/A
4	6.07	5	15.36	13.11	3.5
5	4.14	7	11.48	11.39	5.5
6	5.88	5	7.29	3.34	N/A
7	7.90	2	18.20	11.65	4
8	5.11	6	14.79	5.98	6
9	6.94	3.5	10.56	8.50	6
10	5.59	5.5	6.56	6.09	N/A
11	6.94	3.5	13.87	5.61	6
12	7.13	3	8.86	8.20	7
13	6.55	4	13.65	12.20	3.5
14	5.49	5.5	10.98	10.90	5.5
15	6.55	4	12.23	9.98	5.5
16	6.07	5	14.94	14.38	3
17	6.65	4	10.60	10.03	6
18	4.43	7	11.18	9.54	6
19	6.55	4	10.60	10.50	6
20	6.74	3.5	14.10	13.49	1.5
21	5.39	5.5	16.69	16.59	N/A
22	3.66	N/A	12.04	9.06	6
23	6.26	4.5	13.14	11.77	4.5
24	6.84	3.5	13.08	13.01	4
25	5.78	5			
26	6.74	3.5			
27	3.76	N/A			
28	5.20	6			
29	7.03	3			
30	6.74	3.5			
31	3.18	N/A			
32	5.88	5			
33	4.62	6.5			
34	6.84	3.5			
35	6.17	4.5			
36	4.24	7			
37	2.99	N/A			
38	4.82	6.5			
39	4.43	7			
40	4.34	7			
41	4.62	6.5			
42	3.37	N/A			
43	5.01	6			
44	3.47	N/A			
45	3.08	N/A			
46	3.66	N/A			
47	3.56	N/A			
48	3.18	N/A			
49	3.39	N/A			

TABLE S10. Charged particle track measurements made for the first experimental run. N/A represents measurements that could not be easily fit.

	Run 2 Etch 7 Nov 2019				
	Pd:5521221				
			R2 TRACKS		
	radius	E	major axis	minor axis	E
1	6.74	1	9.97	8.01	6.5
2	5.68	5	15.07	11.57	4
3	7.61	2	12.33	11.33	4.5
4	7.37	1.5	14.58	13.56	3
5	4.24	7	11.53	11.35	5
6	5.01	6	10	9.78	6
7	4.14	7	13.89	13.72	3
8	9.83	N/A	19.91	16.27	N/A
9	5.03	6	9.55	9.43	6.5
10	7.03	3	16.17	15.61	N/A
11	8.29	N/A	10.88	10.1	5.5
12	7.03	3	20.76	17.98	N/A
13	8.38	N/A	18.68	16.46	N/A
14	8.00	2	14.63	12.12	4
15	8.77	N/A	14.04	11.79	4
16	5.01	6	18.72	16.95	N/A
17	4.34	7	11.33	10.49	5.5
18	3.85	N/A	12.26	10.29	5
19	5.01	6	16.19	8.04	5
20	9.25	N/A	16.02	13.01	3
21	7.80	2	16.6	15.61	N/A
22	6.55	3.5	18.26	18.14	N/A
23	8.09	N/A	10.39	7.92	6.5
24	6.55	3.5	14.86	14.43	2.5
25	8.67	N/A	9.81	7.5	6.5
26	8.09	2	15.5	12.84	3
27	5.81	4.5	14.31	13.01	3.5
28	8.29	N/A	14.39	11.98	4
29	6.27	4			
30	3.96	7			
31	4.91	6			
32	6.36	4			
33	6.18	4.5			

TABLE S11. Charged particle track measurements made for the second experimental run. N/A represents measurements that could not be easily fit.

		Run 3 Etch 6 Dec 2019					
		Pd:5521405					
			R3 TRACKS				
	radius	E (MeV)		major axis	minor axis	E	
1	4.14	5	os bot	6.38	5.12	6	ns mid 2
2	5.01	3.5	os bot	9.27	8.59	4.5	os bot
3	5.78	2.5	os bot	9.65	8.25	4.5	os bot
4	4.05	5	os bot	9.95	9.12	4	os bot
5	4.91	4	os bot	10.23	9.88	1	os bot
6	6.84	N/A	nside bot	8.68	7.13	1	os bot
7	6.84	N/A	ns bot	7.05	6.66	1	os bot
8	4.53	4.5	ns bot	8.1	7.07	5.25	os bot 6
9	5.3	3	ns bot	7.61	6.94	5.5	os mida
10	3.87	5.25	ns bot 2	12.99	10.39	3	os mida2bel
11	4.98	3.5	ns bot 2	10.52	9.78	3.5	os mid b
12	1.01	N/A	ns bot 2	13.92	12.2	N/A	os mid b
13	5.81	2.5	ns bot 2	12.25	11.29	2	os mid b
14	6.45	N/A	ns bot 1	11.76	10.79	3	os mid b
15	3.96	5	ns bot 1	13.97	13.16		os mid b
16	4.88	4	ns bot 1	15.97	14.96		os mid b
17	6.54	N/A	ns bot 1	14.6	13.84		os mid b
18	5.35	1	ns bot 4				
19	3.13	6	ns bot 4				
20	6.08	2	ns bot 4				
21	3.85	5.25	os bot				
22	3.85	5.25	os bot				
23	5.3	3	os bot				
24	4.05	5	os bot				
25	3.08	6	os bot				
26	4.62	4.5	os bot				
27	4.53	4	os bot				
28	3.18	6	os bot				
29	3.85	5.25	os bot				
30	4.05	5	os bot 6				
31	4.72	4	os bot 6				
32	5.97	2	os mid b				
33	5.3	3	os mid b				
34	4.91	4	os mid b				
35	5.59	3	os mid b				
36	4.91	4	os mid b				
37	2.86	6.5	os bot 17				
38	5.2	3.5	os t cov				
39	7.42	N/A	os thm 3				
40	3.37	6	os thm 3				
protons							
	1.54	N/A	os thm 3		possible tracks		
	1.16	N/A	os thm 3		os below middle		
	1.35	N/A	os thm 3				
	1.64	N/A	os thm 3				
	1.73	N/A	os thm 3				
	1.93	N/A	os thm 3				

TABLE S12. Charged particle track measurements made for the third experimental run. N/A represents measurements that could not be easily fit.